

## Supplementary Materials

### **Precipitation-assisted heterostructure in a FeMnCoCrCuC high entropy alloy enables superior mechanical property**

**Ye Yuan<sup>1</sup>, Jie Min<sup>1</sup>, Haizheng Pan<sup>1</sup>, Jiajun Wang<sup>1</sup>, Yuliang Yang<sup>1</sup>, Mingwei Zhu<sup>2</sup>, Weiye Chen<sup>3</sup>, Nan Jia<sup>1</sup>**

<sup>1</sup>Key Laboratory for Anisotropy and Texture of Materials (Ministry of Education), School of Materials Science and Engineering, Northeastern University, Shenyang 110819, Liaoning, China.

<sup>2</sup>School of Materials Science and Engineering, Shenyang Aerospace University, Shenyang 110136, Liaoning, China.

<sup>3</sup>School of Materials Science and Engineering, North Minzu University, Yinchuan 750021, Ningxia, China.

**Correspondence to:** Prof. Nan Jia, Key Laboratory for Anisotropy and Texture of Materials (Ministry of Education), School of Materials Science and Engineering, Northeastern University, No. 3-11 Wenhua Road, Heping District, Shenyang 110819, Liaoning, China. E-mail: jian@atm.neu.edu.cn; Prof. Mingwei Zhu, School of Materials Science and Engineering, Shenyang Aerospace University, No.37 Daoyi South Avenue, Shenbei New Area, Shenyang 110136, Liaoning, China. E-mail: mwzhu@sau.edu.cn

## Supplementary figures

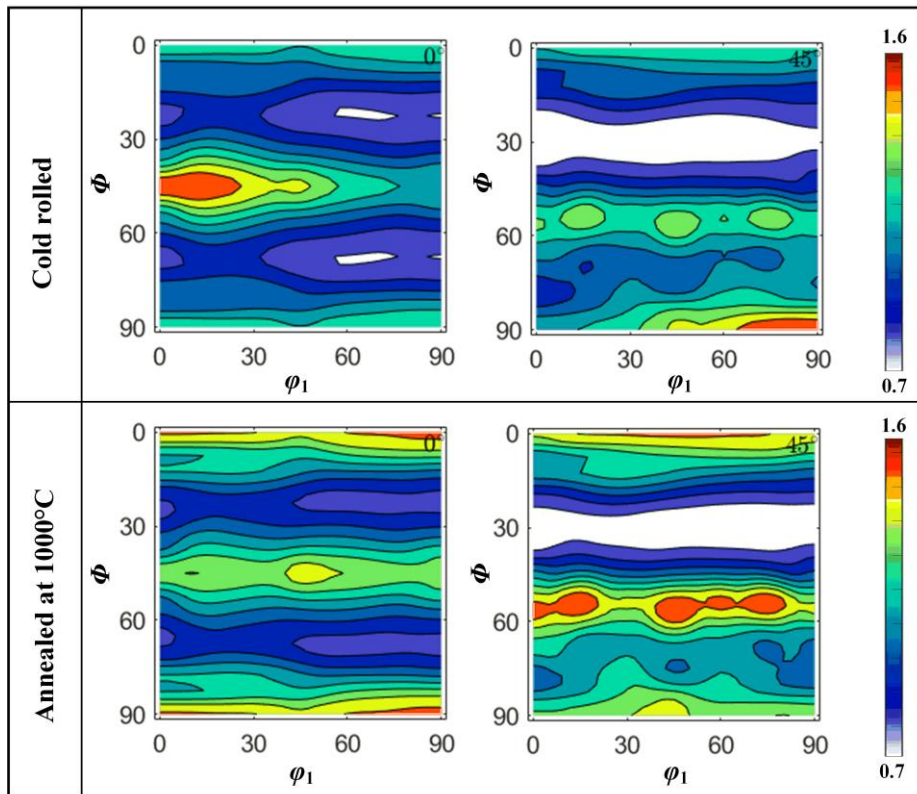


**Fig. S1.** Orientation distribution function (ODF) maps of the C1 alloy in both cold rolled and annealed conditions at  $\phi_2=0^\circ$  and  $45^\circ$ .

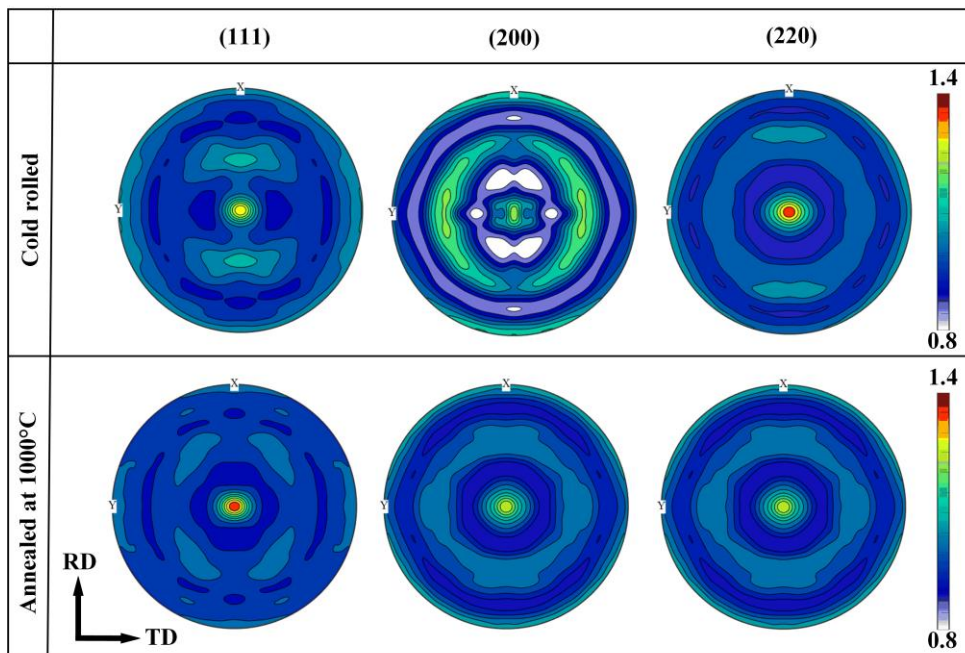


**Fig. S2.** Pole figures (PFs) for the C1 alloy in both cold rolled and annealed states. RD: rolling direction, TD: transverse direction.

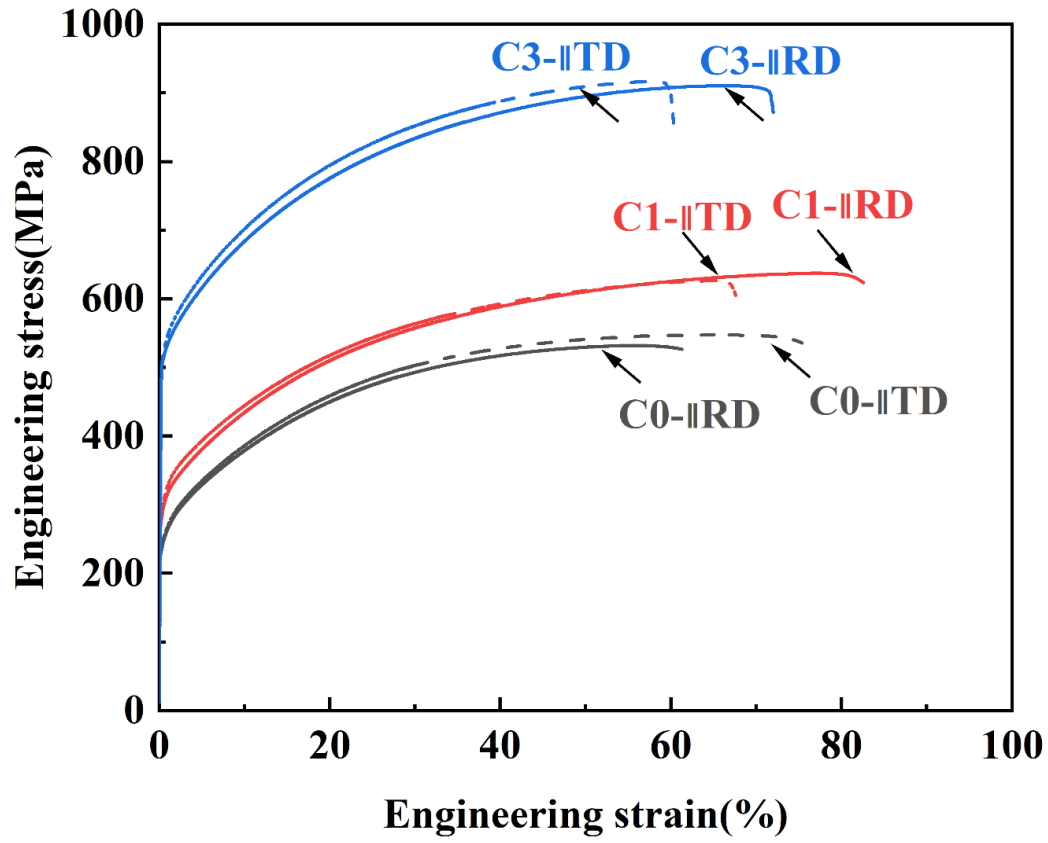


**Fig. S3.** Engineering stress-strain curves of the alloys under uniaxial tension along RD and TD directions.

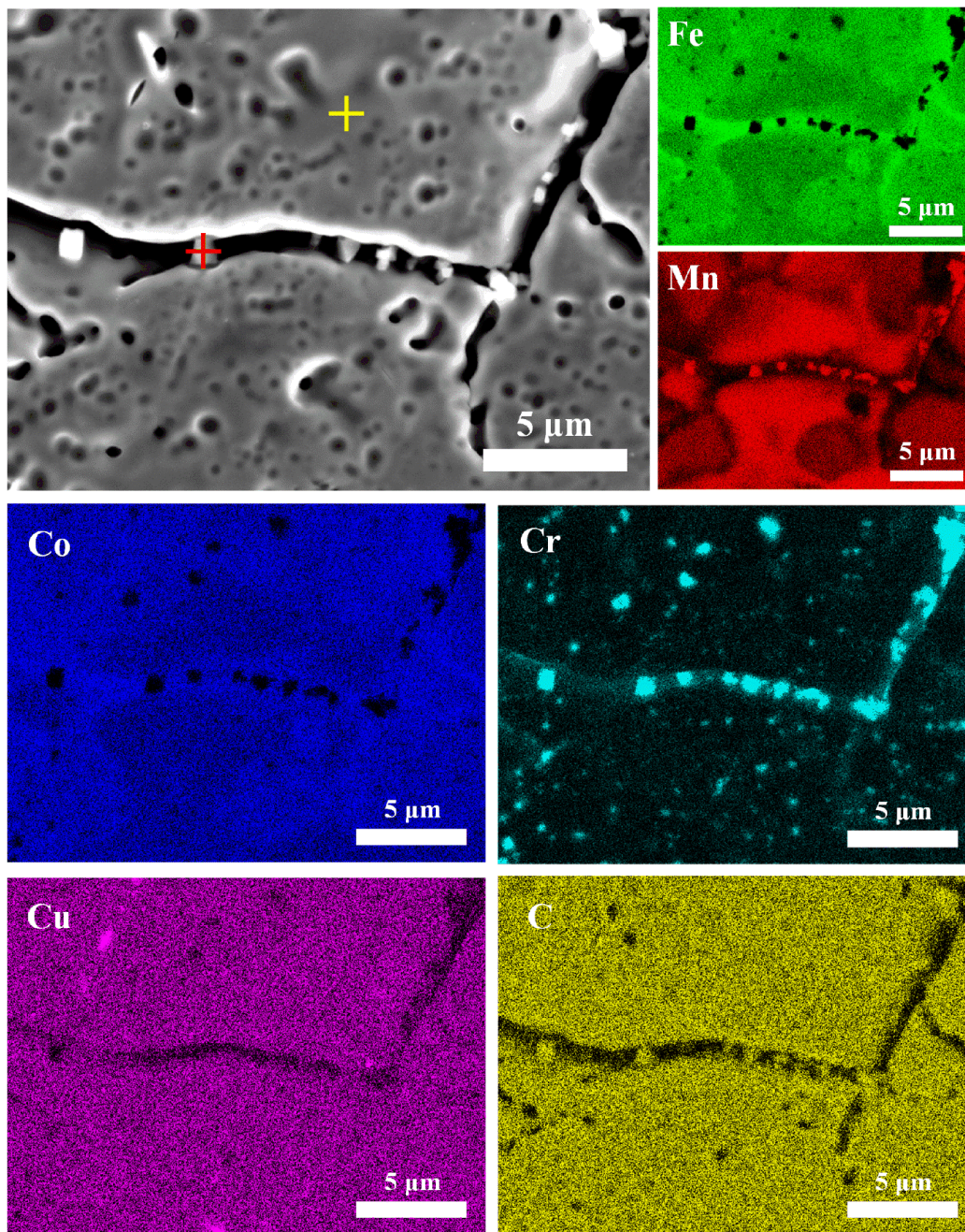


**Fig. S4.** Microstructure and elemental distribution maps of the grain boundary at the triple junction of the C3 alloy, with **Table S2** showing the specific compositions of the matrix and the precipitates at the locations marked in yellow and red crosses, respectively.

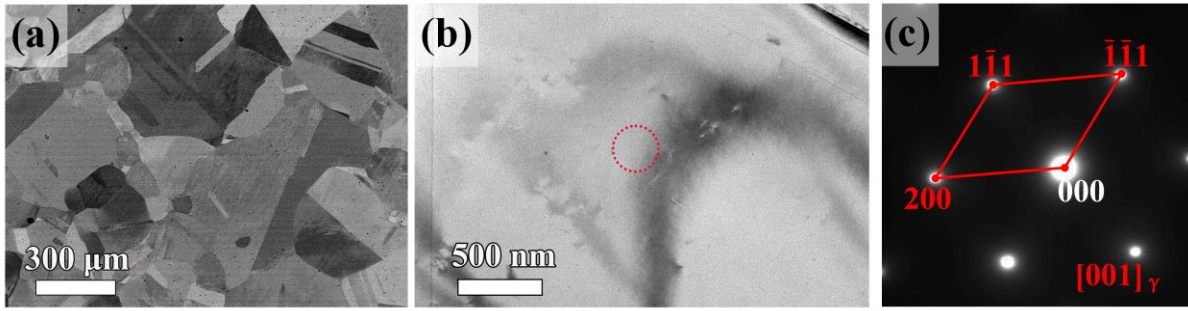


**Fig. S5.** Microstructure of the C3 alloy before cold rolling (at the homogenized state): (a) SEM image, (b) TEM image and (c) the corresponding SAED pattern.

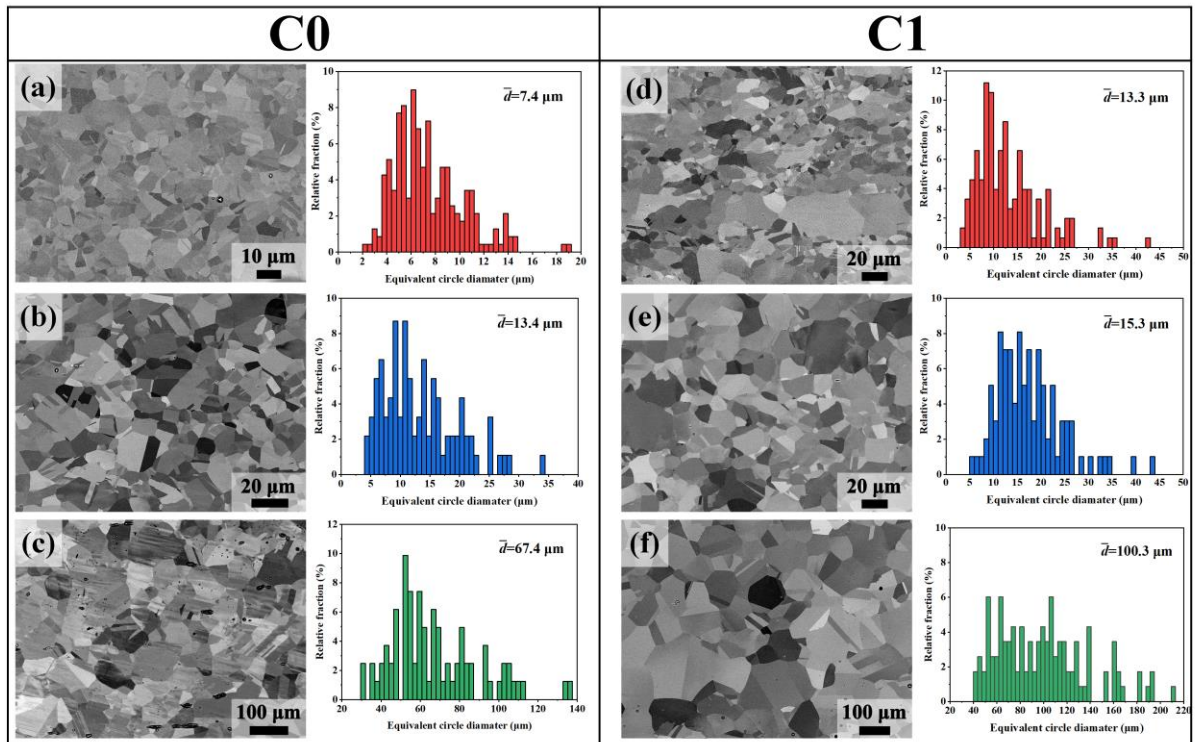


**Fig. S6.** Microstructures and corresponding grain size distributions of C0 and C1 alloys: (a-c) C0 alloy with average grain sizes of 7.4, 13.4, and 67.4  $\mu\text{m}$ ; (e-f) C1 Alloy with average grain sizes of 13.3, 15.3, and 100.3  $\mu\text{m}$ .

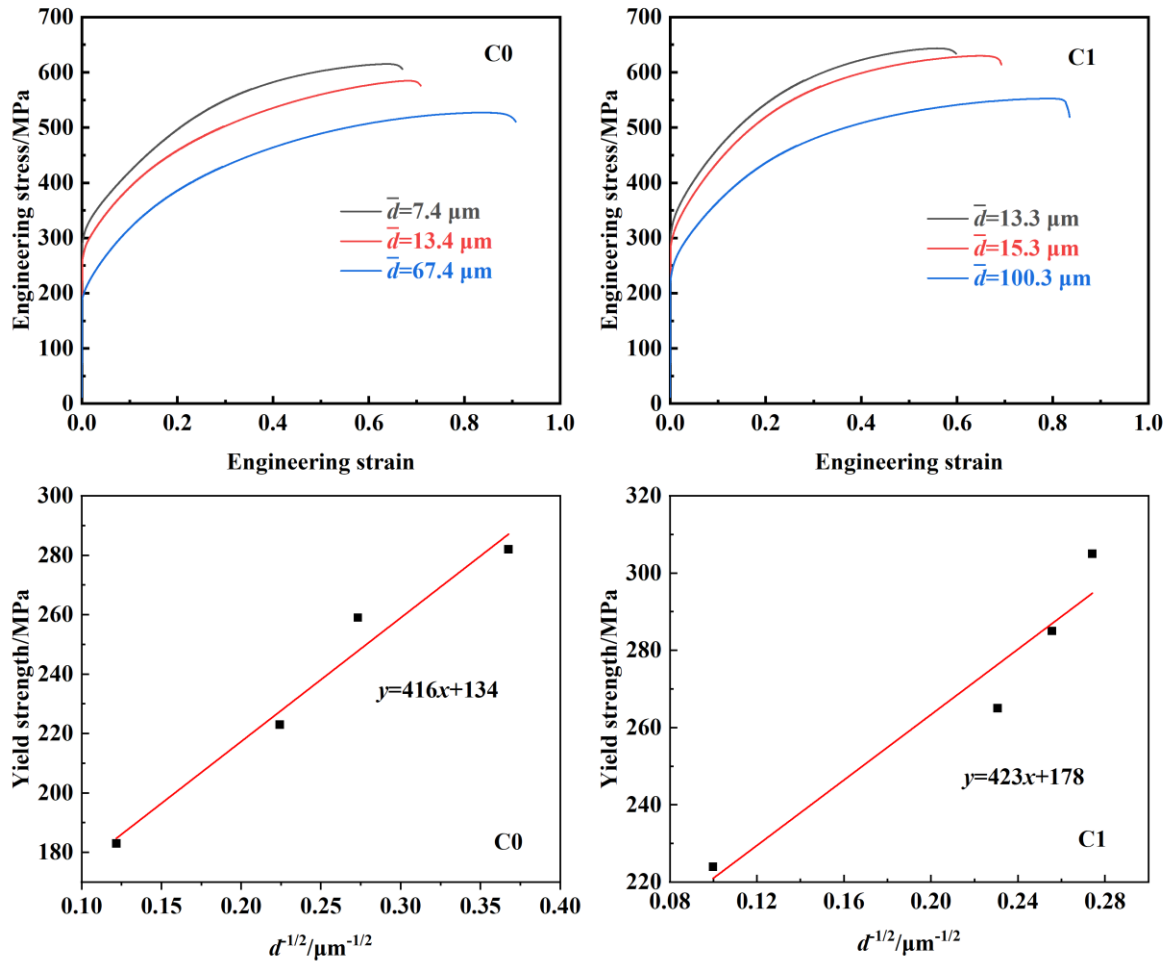


**Fig. S7.** Tensile properties and Hall-Petch fitting curves of C0 and C1 alloys with different grain sizes.

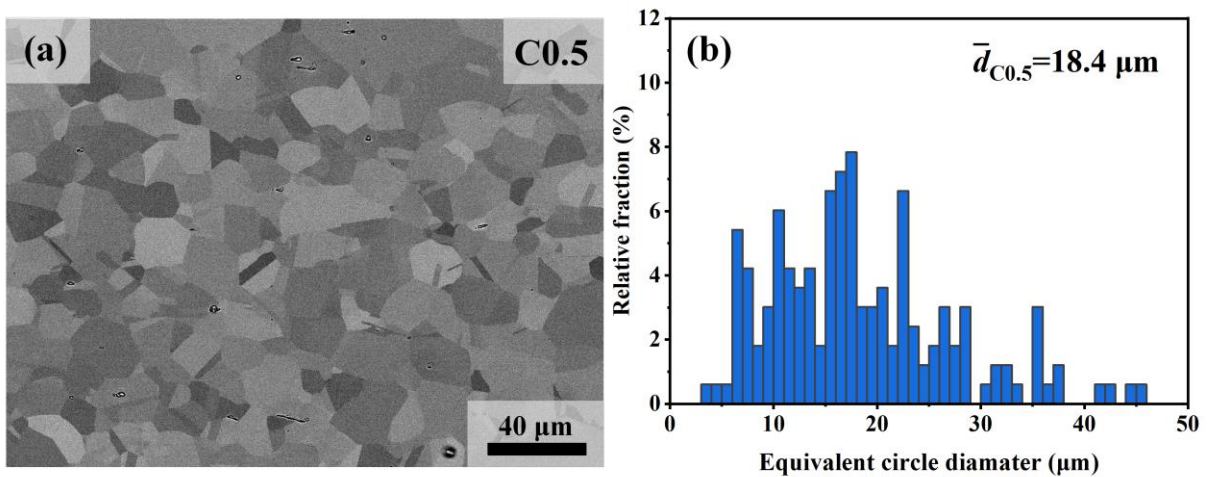


**Fig. S8.** Microstructure of the C0.5 alloys annealed: (a) SEM image, (b) the corresponding grain size distribution.

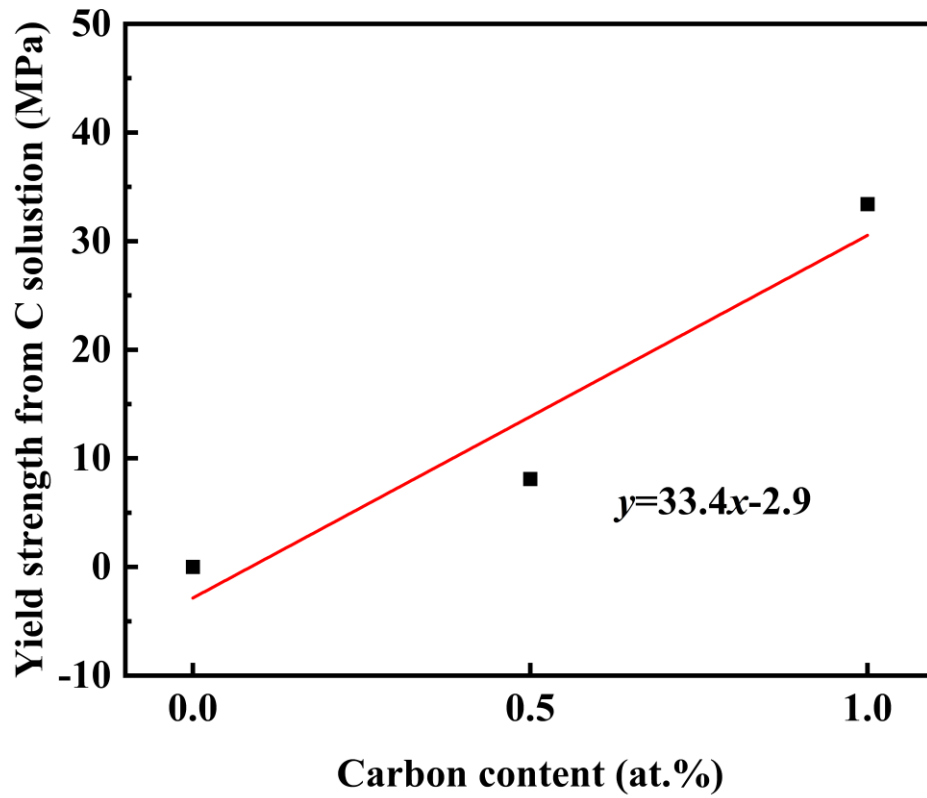


Fig. S9. Strengthening induced by C solution as a function of C content.

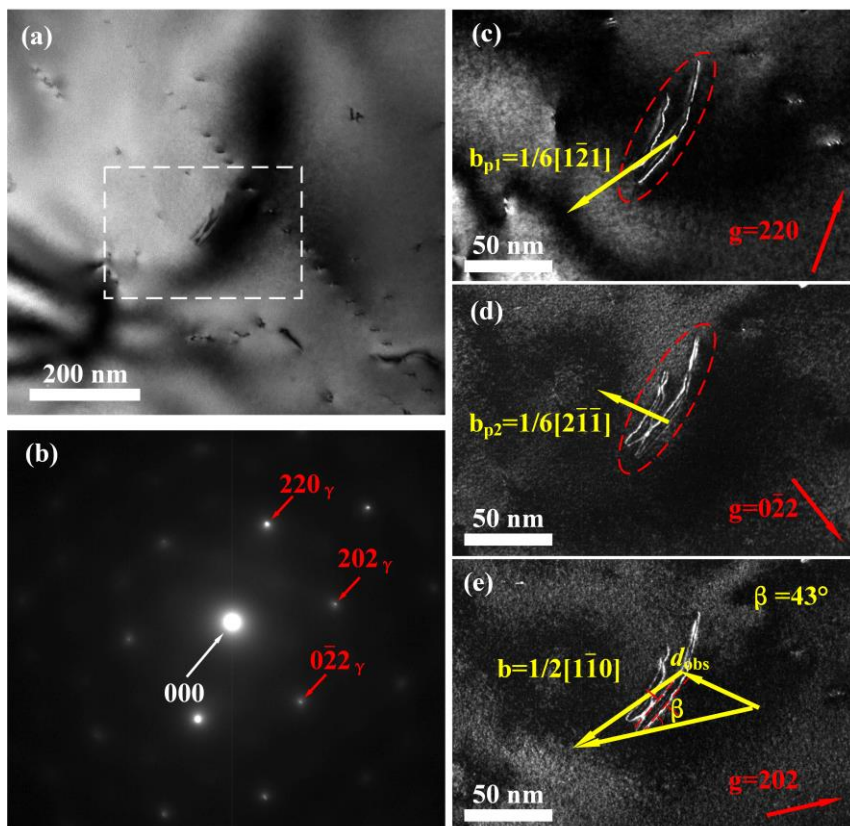


Fig. S10. Dislocation analysis of the C3 alloy before cold rolling (at the homogenized state).

(a) TEM micrograph showing dislocation morphology, (b) diffraction pattern confirming that the  $[111]_{\gamma}$  zone axis is parallel to the incident beam, and (c)-(e)  $g(3g)$  weak beam micrographs extracted from the region indicated by the white dashed rectangle in (a).

### Supplementary table

**Table S1** Tensile properties including  $\sigma_s$ ,  $\sigma_b$ , and  $\varepsilon$  of the C0, C0.5, C1, C2 and C3 alloys.

Alloy	C0	C0.5	C1	C2	C3
$\sigma_s$ (MPa)	223±11	240±9	265±13	417±20	500±22
$\sigma_b$ (MPa)	535±21	566±19	626±30	856±37	979±33
$\varepsilon$ (%)	57.1±5.1	47.6±4.3	49.7±4.7	38.1±3.2	42.0±3.4

This part is footer.  $\sigma_s$ : yield strength;  $\sigma_b$ : tensile strength;  $\varepsilon$ : uniform elongation.

**Table S2** Compositions of the matrix and precipitates shown in Fig. S4.

Contents (at.%)	Fe	Mn	Co	Cr	Cu	C
Matrix	48.5±0.63	27.17±0.4 1	9.61±0.10	9.58±0.11	3.10±0.07	2.29±0.32
Precipitate	23.18±1.3 6	23.94±2.6 7	3.92±0.19	42.35±0.8 9	0.87±0.08	5.74±0.44

## Supplementary notes

### (I) Texture analysis

To analyze the texture evolution in both rolled and the subsequently annealed samples, we conducted orientation analysis using the C1 alloy as an example. The orientation distribution function (ODF) maps and pole figures (PFs) are shown in **Supplementary Figures 1 and 2**, respectively. The ODF maps indicate that both the rolled and annealed samples exhibit very weak mixed textures. Specifically, the rolled samples show Goss and Brass textures, while the annealed samples retain these textures and also develop the Cube texture. The PFs show very low intensity, revealing a weak {111} texture aligned with the normal direction (ND) of the sheet in both the rolled and annealed states.

To further investigate the influence of texture on the tensile properties (anisotropy in mechanical property) of the alloys, we conducted mechanical testing on C0, C1, and C3 alloy samples processed by annealing at 1000°C for 3 min, with tensile direction parallel to transverse direction (TD) and rolling direction (RD), respectively. It should be noted that due to the sample thickness of only 1 mm, samples could not be prepared parallel to ND. Additionally, the dimensions of these samples differ slightly from those described in the main text, which may result in minor deviations in tensile properties from those reported in manuscript. The mechanical properties of the three alloys along RD and TD are shown in **Supplementary Figure 3**, indicating insignificant differences in mechanical properties between the different sample directions.

### (II) SFE calculation

The stacking fault energy (SFE) of the solution-treated C3 alloy is calculated using the following formula<sup>[1]</sup>:

$$\gamma_{\text{sf}} = \frac{Gb_p^2}{8\pi d_{\text{act}}} \left( \frac{2-\nu}{1-\nu} \right) \left( 1 - \frac{2\nu \cos(2\beta)}{2-\nu} \right) \quad (1)$$

where  $\gamma_{\text{sf}}$  is the SFE,  $G$  is the shear modulus (referenced to Fe<sub>49.5</sub>Mn<sub>30</sub>Co<sub>10</sub>Cr<sub>10</sub>C<sub>0.5</sub> alloy, ~76 GPa<sup>[2]</sup>),  $\beta$  is the angle between the dislocation line and the Burgers vector of the full dislocation,  $\mathbf{b}$  is Burgers vector, determined using the  $\mathbf{g} \cdot \mathbf{b} = 0$  method (as shown in

**Supplementary Figure 4**),  $\mathbf{g}$  is the diffraction vector,  $b_p$  is the magnitude of the Burgers vector of the Shockley partial dislocation (calculated from the lattice constant of the C3 alloy, 0.148 nm),  $\nu$  is the Poisson's ratio (Cantor alloy, 0.26<sup>[3]</sup>), and  $d_{\text{act}}$  is the actual stacking fault (SF) width (the distance between two Shockley partial dislocations). The value of  $d_{\text{act}}$  is obtained by correcting the observed SF width ( $d_{\text{obs}}$ ) using following equations:

$$d_{\text{act}} = \sqrt{a_{\text{obs}}^2 - \frac{4}{ab}} + \frac{b-a}{ab} \quad (2)$$

$$a = \frac{-s_g}{\frac{\mathbf{g}}{2\pi} \cdot (\mathbf{b}_{p1} + \frac{\mathbf{b}_{p1,e}}{2(1-\nu)})} \quad (3)$$

$$b = \frac{-s_g}{\frac{\mathbf{g}}{2\pi} \cdot (\mathbf{b}_{p2} + \frac{\mathbf{b}_{p2,e}}{2(1-\nu)})} \quad (4)$$

In the formula,  $\mathbf{b}_{p1}$ ,  $\mathbf{b}_{p2}$ ,  $\mathbf{b}_{p1,e}$  and  $\mathbf{b}_{p2,e}$  are the Burgers vectors of the Shockley partial dislocations and their edge dislocation components, respectively;  $s_g$  is the excitation error in electron beam diffraction, which can be obtained through equation (5):

$$s_g = \frac{1}{2} (n-1) |\mathbf{g}|^2 \lambda \quad (5)$$

where  $\lambda$  is the electron wavelength. The weak beam uses  $\mathbf{g}$  ( $3\mathbf{g}$ ) to ensure that  $\mathbf{g} \cdot \mathbf{b} \leq 2$ . The acceleration voltage selected for this experiment is 200 kV, resulting in an  $s_g$  of  $\sim 0.15 \text{ nm}^{-1}$ . Three  $\langle 110 \rangle$   $\mathbf{g}$  vectors are selected on the [111] zone axis to determine the Burgers vector directions of the Shockley partial dislocations and the full dislocations, as shown in the **Supplementary Figure 4**. According to **Supplementary Figures 4c-e**,  $\beta$  is determined to be  $43^\circ$ , and  $d_{\text{act}}$  is  $4.1 \pm 1.7 \text{ nm}$ . Ultimately, the SFE of the C3 alloy is calculated to be  $37.2 \pm 10.9 \text{ mJ} \cdot \text{m}^{-2}$ .

## References

- [1] Laplanche G, Kostka A, Reinhart C, Hunfeld J, Eggeler G, et al. Reasons for the superior mechanical properties of medium-entropy CrCoNi compared to high-entropy CrMnFeCoNi. *Acta Mater.*, 2017; 128: 292-303. [DOI: 10.1016/j.actamat.2017.02.036]
- [2] Su J, Raabe D, Li Z M. Hierarchical microstructure design to tune the mechanical behavior of an interstitial TRIP-TWIP high-entropy alloy. *Acta Mater.*, 2019; 163: 40-54. [DOI: 10.1016/j.actamat.2018.10.017]
- [3] Wu Z G, Bei H B, Pharr G M, George E P. Temperature dependence of the mechanical properties of equiatomic solid solution alloys with face-centered cubic crystal structures. *Acta Mater.*, 2014; 81: 428-441. [DOI: 10.1016/j.actamat.2014.08.026]